

**Citation for published version:**

Xiaorun Zhou, et al, 'Surface Morphology Evolution Mechanisms of InGaN/GaN Multiple Quantum Wells with Mixture N<sub>2</sub>/H<sub>2</sub>-Grown GaN Barrier', *Nanoscale Research Letters*, (2017) 12:354.

**DOI:**

<http://dx.doi.org/10.1186/s11671-017-2115-8>

**Document Version:**

This is the Published Version.

**Copyright and Reuse:**

© 2017 The Author(s).

This is an Open Access article is distributed under the terms of the Creative Commons Attribution 4.0

International License

( <http://creativecommons.org/licenses/by/4.0/> ), which

permits unrestricted use, distribution, and

reproduction in any medium, provided you give appropriate credit to the original author(s) and the source, provide a link to the Creative Commons license, and indicate if changes were made.

**Enquiries**


If you believe this document infringes copyright, please contact the Research & Scholarly Communications Team at [rsc@herts.ac.uk](mailto:rsc@herts.ac.uk)

NANO EXPRESS

Open Access



# Surface Morphology Evolution Mechanisms of InGaN/GaN Multiple Quantum Wells with Mixture N<sub>2</sub>/H<sub>2</sub>-Grown GaN Barrier

Xiaorun Zhou<sup>1,2</sup>, Taiping Lu<sup>1,2\*</sup> , Yadan Zhu<sup>1,2</sup>, Guangzhou Zhao<sup>1,2</sup>, Hailiang Dong<sup>1</sup>, Zhigang Jia<sup>1,2</sup>, Yongzhen Yang<sup>1,2\*</sup>, Yongkang Chen<sup>1</sup> and Bingshe Xu<sup>1,2</sup>

## Abstract

Surface morphology evolution mechanisms of InGaN/GaN multiple quantum wells (MQWs) during GaN barrier growth with different hydrogen (H<sub>2</sub>) percentages have been systematically studied. Ga surface-diffusion rate, stress relaxation, and H<sub>2</sub> etching effect are found to be the main affecting factors of the surface evolution. As the percentage of H<sub>2</sub> increases from 0 to 6.25%, Ga surface-diffusion rate and the etch effect are gradually enhanced, which is beneficial to obtaining a smooth surface with low pits density. As the H<sub>2</sub> proportion further increases, stress relaxation and H<sub>2</sub> over-etching effect begin to be the dominant factors, which degrade surface quality. Furthermore, the effects of surface evolution on the interface and optical properties of InGaN/GaN MQWs are also profoundly discussed. The comprehensive study on the surface evolution mechanisms herein provides both technical and theoretical support for the fabrication of high-quality InGaN/GaN heterostructures.

**Keywords:** GaN barrier, Hydrogen, Surface, Interface

## Background

InGaN/GaN-based high-brightness light-emitting diodes (LEDs) and laser diodes, as the representative devices of III-nitrides, have attracted much attention owing to their important role in digital signage, high-density optical storage, and general illumination [1–10]. Generally speaking, fabrication of blue or green LEDs requires relatively high indium composition of InGaN layer [11, 12]. Although the reduction of growth temperature and the increase of growth rate of the quantum well (QW) can alleviate indium atom desorption to obtain high indium content, these methods also deteriorate the optical performance of InGaN/GaN multiple quantum wells (MQWs) by worsening interface abruptness and introducing more defects [13, 14]. Moreover, these defects usually act as nonradiative recombination centers, thus weakening the internal quantum efficiency of the device [15–19]. Therefore, achieving required indium

content while maintaining high material quality is still a big challenge.

In order to settle the problems mentioned above, various growth techniques have been employed in striving for smooth morphology and sharp interfaces within the InGaN/GaN stack. Quantum barriers (QBs) grown at elevated temperature [20, 21] and growth interruption after QWs [12, 22] are widely used to improve the morphology of InGaN/GaN heterostructures. However, they all have their own limitations. For instance, barriers grown at high temperature may lead to severe In loss [14, 23]. Although growth interruption can improve morphology as well as reduce inclusions, it is at the expense of the optical quality of the QWs [21]. Recently, it is reported that introducing a small amount of hydrogen during the growth of GaN barriers can improve both optical and interface properties [24–28]. However, the effect mechanism of H<sub>2</sub> on surface evolution of InGaN/GaN MQWs has not been fully understood yet.

In this paper, the effects of H<sub>2</sub> proportion, defined as H<sub>2</sub> flow divided by total carrier gas flow, during GaN barrier deposition, on surface morphology evolution are systematically investigated. Ga surface-diffusion rate,

\* Correspondence: [lutaiping@tyut.edu.cn](mailto:lutaiping@tyut.edu.cn); [yyztyut@126.com](mailto:yyztyut@126.com)

<sup>1</sup>Key Laboratory of Interface Science and Engineering in Advanced Materials, Ministry of Education, Taiyuan University of Technology, Taiyuan 030024, China

Full list of author information is available at the end of the article

stress relaxation, and H<sub>2</sub> etching effect are suggested to be the three main factors, affecting surface evolution. The dominant factors and their influences on the surface evolution are comprehensively discussed, which provides a technical guideline to obtain high-quality InGaN/GaN heterostructures.

## Methods

The InGaN/GaN MQW structures were grown on *c*-plane sapphire substrate by Aixtron TS300 metal organic chemical vapor deposition system. Trimethylgallium (TMG), triethylgallium (TEG), trimethylindium (TMI), and ammonia (NH<sub>3</sub>) were used as precursors. Silane (SiH<sub>4</sub>) was used as the *n*-type dopant source. The structure was composed of 3.2- $\mu$ m-thick undoped GaN layer and nominally six-period 2.4-nm-thick InGaN QWs separated by 11-nm-thick lightly Si-doped (*n*-doping =  $3 \times 10^{17} \text{ cm}^{-3}$ ) GaN barriers. A 1.0-nm-thick low temperature GaN cap layer (LT-GaN) was deposited immediately after the growth of QW layer. InGaN wells and GaN barriers were grown at 730 and 850 °C, respectively. A conventional InGaN/GaN MQWs sample, labeled as S<sub>1</sub>, was grown in nitrogen atmosphere. Four other samples, denoted as S<sub>2</sub>, S<sub>3</sub>, S<sub>4</sub>, and S<sub>5</sub>, were grown with different proportion of H<sub>2</sub> flow to total carrier gas (N<sub>2</sub> + H<sub>2</sub>) during barriers deposition, with the other growth parameters the same with S<sub>1</sub>. The percentage of H<sub>2</sub> was 2.5% (S<sub>2</sub>), 6.25% (S<sub>3</sub>), 10% (S<sub>4</sub>), and 50% (S<sub>5</sub>), respectively.

The structures of InGaN/GaN MQWs were characterized by PANalytical Empyrean high resolution x-ray diffraction (HRXRD) system. Surface morphology was obtained by atomic force microscopy (AFM) (SPA-300HV) using tapping model. Room temperature (RT) photoluminescence (PL) properties of the samples were studied by 226-nm Nd-YAG laser with an excitation power density of 1.36 W/cm<sup>2</sup>.

## Results and Discussion

The HRXRD  $\omega$ -2 $\theta$  scanning results of S<sub>1</sub>–S<sub>5</sub> are illustrated in Fig. 1a. The strongest peak located at the center belongs to the underlying GaN template, and the satellite peaks correspond to the periodicity of the MQWs. It is found that the full-width at half-maximum (FWHM) of the strongest peaks in all samples is almost the same, indicating the similar crystal quality of GaN buffer layers for all samples. The presence of clearly distinguished “+4th” diffraction peak in samples S<sub>2</sub>–S<sub>4</sub> manifest the improvement of crystal quality under low H<sub>2</sub> percentage. The appearance of the “+5th” diffraction peak (represented by the rectangle in Fig. 1a) and the minimum FWHM value of InGaN “–1st” diffraction peak indicate the best interface quality in sample S<sub>3</sub>. The structure parameters determined by fitting the measured XRD curves are summarized in Table 1. The period thicknesses of the five samples are almost the same, and the values keep around 14.4 nm. The indium contents of the InGaN wells for samples S<sub>1</sub> to S<sub>4</sub> keep around 11.8%, while the value drops to 9.9% for S<sub>5</sub>. A large amount of H<sub>2</sub> may etch the GaN LT-cap layer and then react with indium atoms in QWs, which result in the reduction of average indium content [29]. The roughness of the interface can be calculated by fitting FWHM of the XRD satellite peak by the following equation [26, 30]:

$$\Delta\omega_n = \Delta\omega_0 + \left[ (\ln 2)^{1/2} \cdot \Delta\theta_M \cdot \frac{\gamma}{D} \right] \cdot n \quad (1)$$

where  $\Delta\omega_n$  represents the FWHM of the *n*-th satellite peak,  $\Delta\omega_0$  is the intrinsic width of satellite peaks,  $\Delta\theta_M$  is the angle spacing between the adjacent satellite peaks, *D* is the period thickness of the InGaN/GaN MQW and  $\gamma$  is the interface roughness. Figure 1b shows the linear relationship between FWHMs and satellite peak orders. The slope of the fitting line is related to the QW/QB interface roughness. The fitting results show that

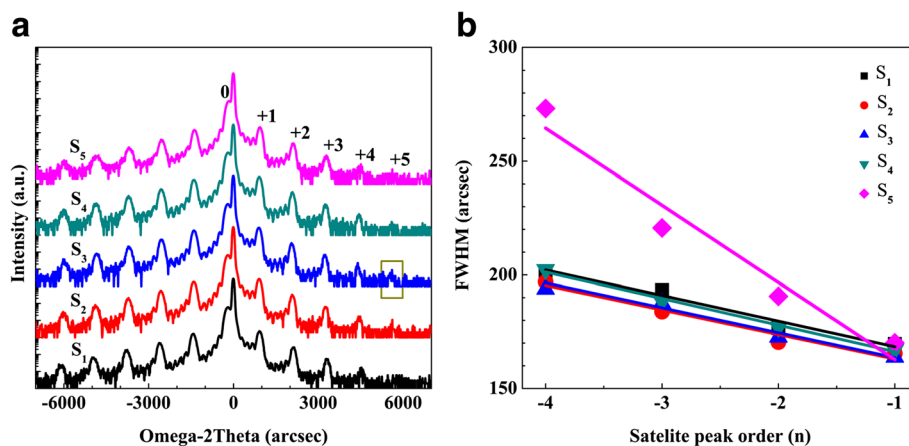


**Fig. 1** a The HRXRD  $\omega$ -2 $\theta$  scanning results of S<sub>1</sub>–S<sub>5</sub>. b The FWHM as a function of the satellite peak order and its linear fitting for the five samples



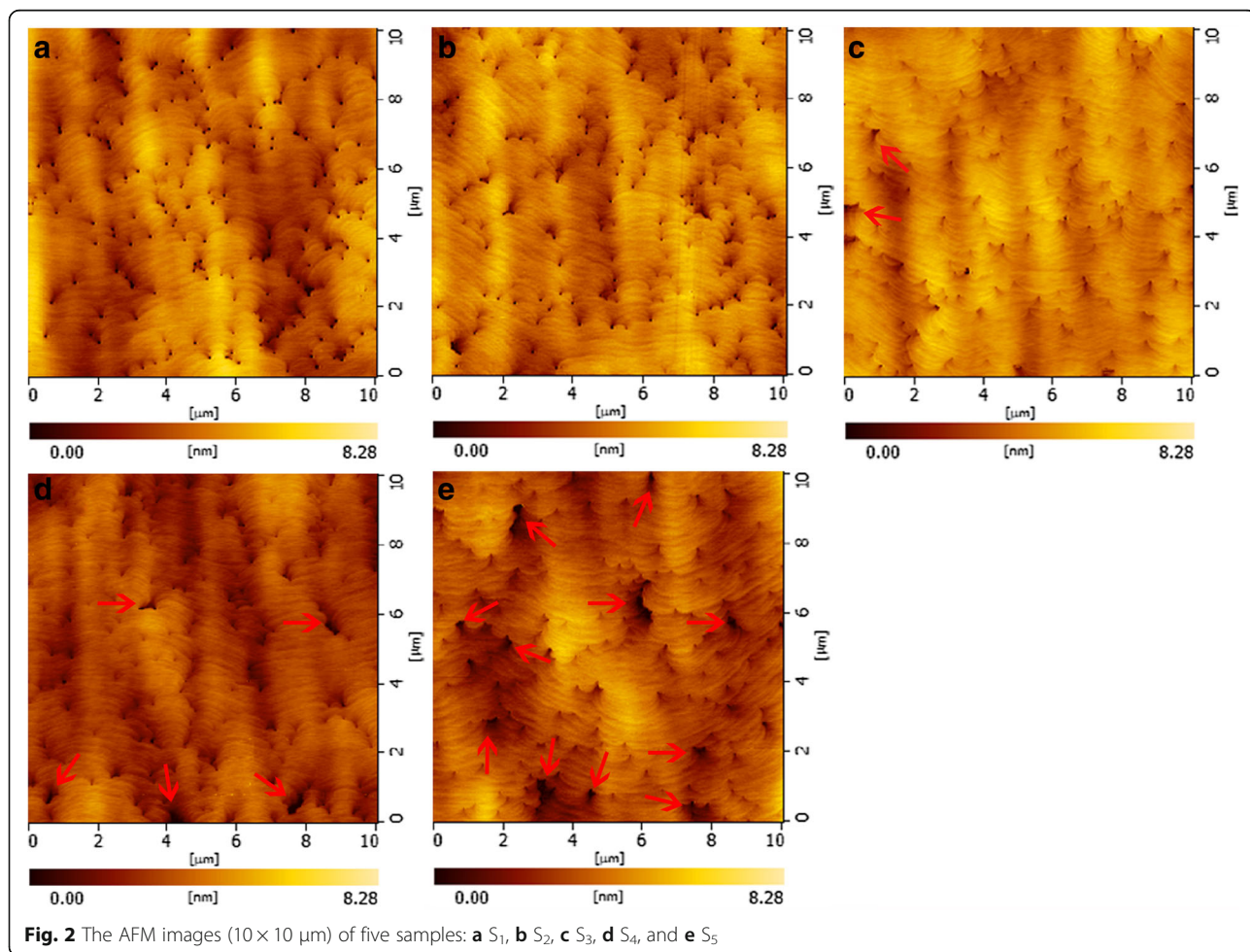
**Table 1** Structure parameters of InGaN/GaN MQWs determined by HRXRD fitting

Sample	H <sub>2</sub> percentage (%)	In content (%)	FWHM of InGaN “-1st” diffraction peak (arcsec)	Slope of liner fitting
S <sub>1</sub>	0	11.84	169.66	-11.27
S <sub>2</sub>	2.50	12.04	165.43	-10.79
S <sub>3</sub>	6.25	11.67	163.77	-10.49
S <sub>4</sub>	10	11.60	167.19	-11.68
S <sub>5</sub>	50	9.90	170.13	-33.92

interface roughness is gradually reduced as the H<sub>2</sub> percentage increases, and the optimum value is achieved at 6.25% of H<sub>2</sub> (S<sub>3</sub>), as shown in Table 1. With further raising in the percentage to 50% (S<sub>5</sub>), the interface roughness is increased dramatically. Hence, the ratio of H<sub>2</sub> during barrier growth has great impact on interface quality. A small percentage (0–6.25%) of H<sub>2</sub> is favorable to obtaining sharp interface, while a large amount of H<sub>2</sub> (50%) seriously roughens the interface.

The AFM images of sample S<sub>1</sub>–S<sub>5</sub> are shown in Fig. 2a–e. The dark points are mainly V-pits [14, 31], which initiate at the threading dislocations (TDs) [21,

27]. The root mean square (RMS) surface roughness under different H<sub>2</sub> percentage is illustrated in Fig. 3. The reference sample S<sub>1</sub> grown with H<sub>2</sub>-free condition possesses the coarsest surface with an RMS roughness of 1.028 nm. The RMS value decreases with the increase of H<sub>2</sub> percentage, and achieves the minimum value (0.705 nm) at 6.25% of H<sub>2</sub>, as shown in Fig. 3. As the H<sub>2</sub> percentage raises to 10%, the surface gets slightly rougher. With further increase in H<sub>2</sub> percentage to 50%, many large holes are formed, as pointed out by red arrows in Fig. 2, and surface RMS roughness dramatically increases to 0.924 nm.



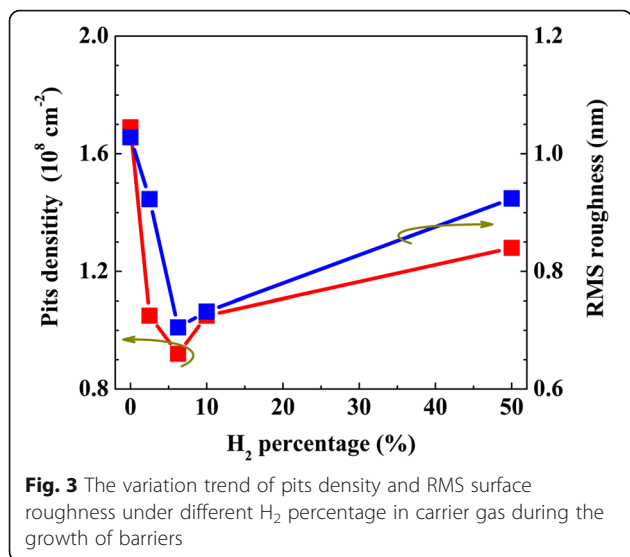
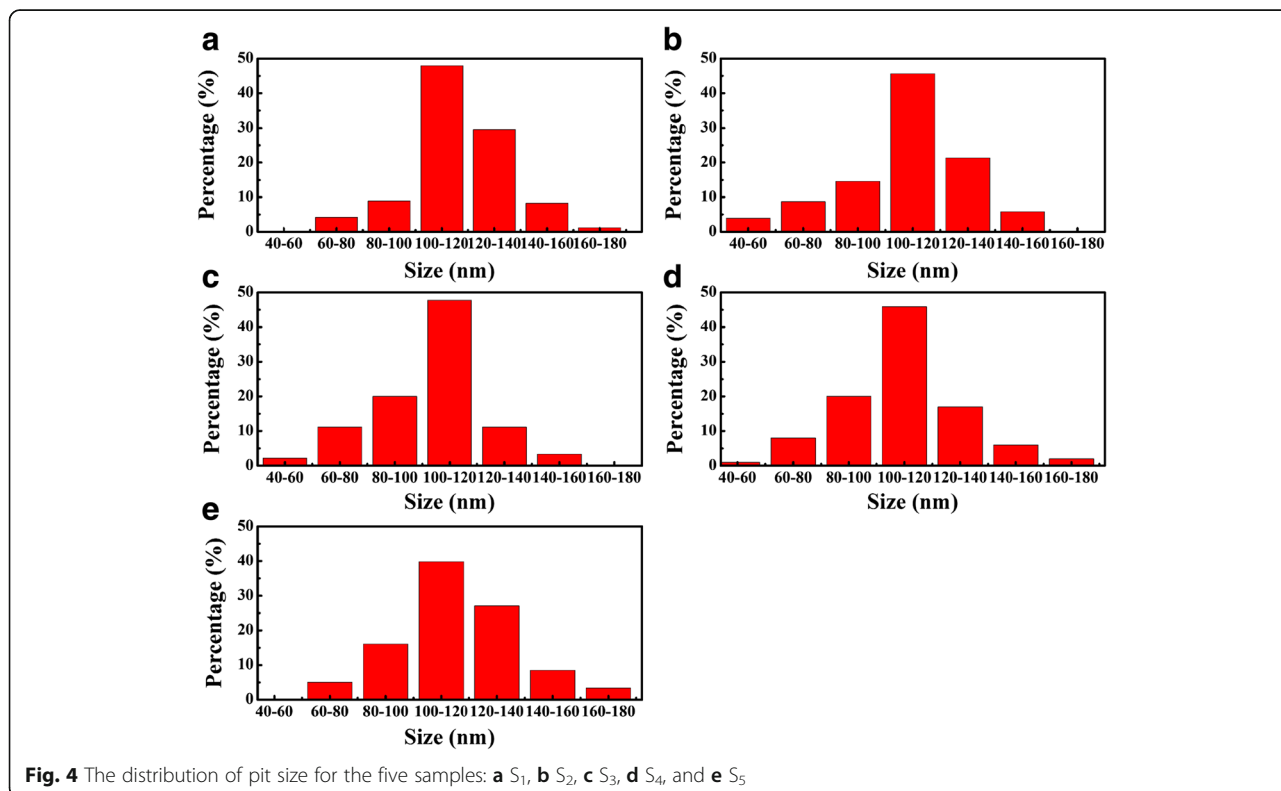


Figure 4 shows the statistical calculated diagram of pits size distributions for the five samples. It can be seen that as 2.5% H<sub>2</sub> is introduced, the smallest pits (<60 nm) start to emerge, and the largest pits (>160 nm) disappear. As H<sub>2</sub> percentage increases to 6.25% (S<sub>3</sub>), the proportion of pits at size 80–100 nm is significantly raised, and that of large pits (>140 nm) is dramatically reduced to the minimum value. With further increase in the H<sub>2</sub> percentage to

10%, the largest pits begin to emerge again. When 50% H<sub>2</sub> is introduced, the ratio of large pits is dramatically increased. Hence, the pits size can be reduced by introducing a small amount of H<sub>2</sub>, and the optimum value is acquired at 6.25% percentage. However, the pits size shows an increase trend as H<sub>2</sub> percentage further rises.

It is obvious that the evolution trend of RMS surface roughness is highly consistent with that of pits size, which may relate to the growth mode affected by the formed pits. Once the pits are formed, indium atoms will first nucleate at the point where the TDs intersect the InGaN/GaN interface [32–35], then island growth starts and finally island growth mode transfers to 2-Dimensional growth. In other words, the presence of V-pits will delay the 2-dimensional growth, then roughen the surface. The larger the size is, the more obvious the delay can be.

In order to elucidate the surface evolution mechanism under different H<sub>2</sub> percentages, the variation trend of V-pits size is discussed in detail. As H<sub>2</sub> percentage increases from 0 to 6.25%, the decrease in V-pits size possibly comes from the following two parts. First, the formed Ga-H complex may enhance the incorporation efficiency of Ga atoms on {10 $\bar{1}$ 1} plane [35]. It is reported that the adsorption energy of the Ga-H complex is about 1.2 eV smaller than that of single Ga adatoms [28]. Hence, the attachment of hydrogen to Ga adatom could significantly



weaken the bond to the surface, which benefits the surface diffusion of Ga atoms [28, 36]. Another important reason is the gradually enhanced etching effect with the increase of  $H_2$  percentage. Shiojiri et al. reported that indium atoms can be easily trapped and segregated around the core of TDs, which plays a role of a small mask that hinders Ga atoms migration [37]. Hence, introducing  $H_2$  during the growth can effectively eliminate indium-rich clusters at InGaN/GaN interface, and contribute to surface migration of Ga atoms [37–39]. In addition, hydrogen can etch some unstable areas, such as dislocation sites and V-pits [40–43]. It is reported that dislocation sites are unstable due to the high strain energy and weak binding energy, and these sites can be easily dissociated during the etching process [41–43]. Moreover, the V-pit commonly consists of six symmetric N-terminated  $\{10\bar{1}1\}$  facets [44, 45], which is much weaker during the etching process as compared with Ga-terminated facets [42, 43]. Therefore, when  $H_2$  arrives at the surface, it is difficult to etch most of the GaN on the surface due to the high stability of Ga-face. Thus,  $H_2$  etching occurs mainly at dislocation sites and V-pits [42, 43], causing the decomposition of GaN. Due to the low growth temperature of GaN barrier, the decomposition effect of GaN is weak when hydrogen percentage is low [26]. Hence, the enhanced Ga atoms incorporation plays a dominant role in surface evolution, which is beneficial in reducing the size and density of pits and in turn enhances the 2-Dimensional growth and suppresses the formation of new pits, and finally conducive to smooth surface. The correlation between pits density and  $H_2$  percentage is presented in Fig. 3. It is shown that the highest pit density ( $1.69 \times 10^8 \text{ cm}^{-2}$ ) exists in the  $H_2$ -free sample. While a small amount of  $H_2$  is added in the carrier gas, pits density is gradually reduced and reaches the lowest value ( $0.92 \times 10^8 \text{ cm}^{-2}$ ) in sample  $S_3$ . With further increase in  $H_2$  proportion to 50%, pits density is significantly increased to  $1.28 \times 10^8 \text{ cm}^{-2}$ . These results indicate that adding a little  $H_2$  in the growth of barrier layer can suppress the formation of new pits. However, the suppression of new pits formation could lead to strain accumulation inside the layer, and the strain may relax via formation of new dislocations and other defects such as

big pits in  $S_4$  and  $S_5$  [21], which will deteriorate the quality of the surface, as well as the InGaN/GaN interface.

It is worth to mention that the large holes ( $>200 \text{ nm}$ ) as marked with red arrows do not appear in samples  $S_1$  and  $S_2$ , and they only start to appear as  $H_2$  percentage becomes larger than 2.5%. The hole size in  $S_5$  is much larger than that in samples  $S_3$  and  $S_4$ , which may relate to the following two possible mechanisms about hydrogen over-etching mechanisms. One is the hydrogen over-etching on dislocation sites and V-pits. As aforementioned, the enhanced diffusion of Ga atoms plays a dominant role when hydrogen percentage is low. However, this leading role shifts to the enhanced GaN decomposition around dislocation sites and V-pits when large amounts of hydrogen are applied. The hydrogen can diffuse along the dislocation line and then etch the surrounded unstable sites both vertically and longitudinally, which could decrease the average indium contents in MQWs region, degrade well/barrier interface quality and also form large holes on the surface. Another possible mechanism is about hydrogen over-etching on LT-GaN cap layer. As  $H_2$  proportion lower than 2.5%, the  $H_2$  etch effect on LT-GaN cap layer is negligible. As the  $H_2$  percentage increases to 10%, the  $H_2$  etch effect on LT-GaN cap is illustrated in Fig. 5a.  $H_2$  only etches a part of the cap layer, which has little influence on the QW layer, as evidenced by almost unchanged indium contents, and positive influence on the surface morphology, as confirmed by low pits density and small size of the holes. However, under large  $H_2$  percentage, the LT-GaN cap layer may be partly etched away and QW layer be directly exposed to  $H_2$ , as presented in Fig. 5b. Under this case,  $H_2$  will react with indium atoms in QW layer, leading to significant indium loss, large size, and high-density holes, and consequently dramatically deteriorates InGaN/GaN interface and surface qualities. Hence, surface morphology evolution is an integrated effect of surface diffusion rate, strain relaxation and  $H_2$  etch effect. For sample  $S_2$  and  $S_3$  with  $H_2$  percentage lower than 6.25%, gradually enhanced surface diffusion rate and  $H_2$  etch effect play a dominant role, which contributes to smoother surface and lower pits density. With further

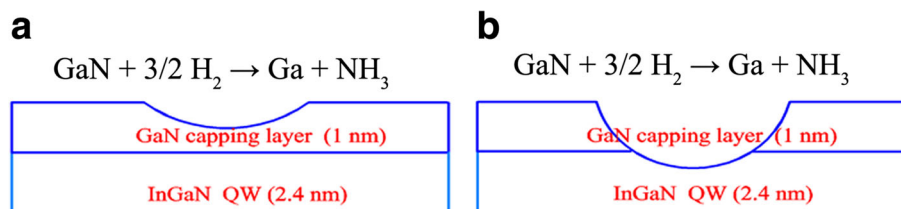
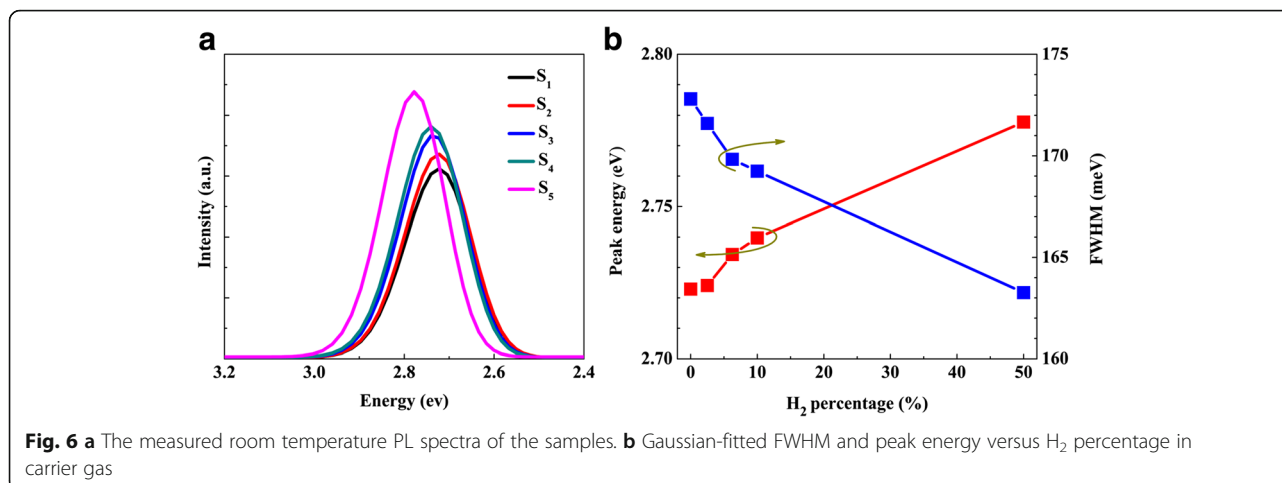


**Fig. 5 a** The etch effect on LT-GaN cap layer with  $H_2$  percentage lower than 10%. **b** the  $H_2$  over etch effect on LT-GaN capping layer under large  $H_2$  percentage



increase in the percentage to 10% ( $S_4$ ), surface properties become slightly worse as a result of stress relaxation. The surface morphology of sample  $S_5$  grown in 50% H<sub>2</sub> is mainly controlled by H<sub>2</sub> over-etching effect and strain relaxation in InGaN QWs, which leads to many large holes and the worst surface.

Figure 6a shows the measured room temperature PL spectra of the five samples. It can be seen that the PL intensity shows an increase trend and peak energy exhibits blue-shift as H<sub>2</sub> percentage increases. Compared with that of sample  $S_1$  without H<sub>2</sub>, the integrated PL intensity of samples  $S_2$ – $S_5$  is increased by 7.0, 15.8, 19.3, and 31.6%, respectively. For samples  $S_2$ – $S_4$ , slightly blue-shifted peak energy and reduced FWHM are observed, as shown in Fig. 6b. As aforementioned, the structure parameters of sample  $S_2$ – $S_4$  are quite similar. Hence, the slightly changed spectral characteristics along with enhanced PL intensity are mainly caused by the enhanced surface and interface quality, and the partial relaxation of stress in QWs alleviating quantum confined stark effect (QCSE) [21, 46]. In contrast, the significantly reduced FWHM, blue-shifted peak energy and enhanced PL intensity of sample  $S_5$  may result from strain relaxation and the lowest indium content caused by H<sub>2</sub> over-etching effect, both of which can greatly alleviate QCSE effect in MQWs [46–49]. In addition, H<sub>2</sub> can eliminate impurities such as carbon and oxygen in active region, which would benefit the improvement of the PL intensity [50, 51].

## Conclusions

In summary, the effect of H<sub>2</sub> percentage during the barriers growth on InGaN/GaN MQWs properties has been systematically studied. As a small percentage of H<sub>2</sub> ( $\leq 6.25\%$ ) is introduced, the combined effect of enhanced H<sub>2</sub> etch effect and surface diffusion contribute to the improvement of surface, interface and optical properties. In

spite of the strongest PL intensity achieved by introducing large percentage H<sub>2</sub> (50%), the integrated effect of H<sub>2</sub> over-etching and stress relaxation degrades surface and interface quality of the InGaN/GaN MQWs. Hence, the use of H<sub>2</sub> with appropriate proportion during the barriers growth can achieve smooth surface with low pits density and enhanced optical performance. The profound discussions of surface evolution mechanism here clearly depict the physical pictures of surface evolution process under different growth conditions, which is helpful for the fabrication of high-quality GaN-based devices.

## Abbreviations

AFM: Atomic force microscopy; HRXRD: High-resolution x-ray diffraction; LED: Light-emitting diode; RMS: Root mean square; PL: Photoluminescence

## Acknowledgements

This work was supported by National Natural Science Foundation of China (Grant Nos. 61504090, 21471111 and 61604104), the Applied Basic Research Projects of Shanxi Province (Grant No. 2016021028), the National Key R&D Program of China (2016YFB0401803), and the Shanxi Provincial Key Innovative Research Team in Science and Technology (Grant No. 201605D131045-10).

## Authors' contributions

XZ and TL conceived the study. XZ, YZ, and GZ conducted the sample-growth and test experiments. TL supervised the entire research project. XZ, TL, YZ, GZ, HD, ZJ, YY, YC, and BX analyzed the data. All authors discussed the results and wrote the manuscript. All authors read and approved the final manuscript.

## Competing interests

The authors declare that they have no competing interests.

## Publisher's Note

Springer Nature remains neutral with regard to jurisdictional claims in published maps and institutional affiliations.

## Author details

<sup>1</sup>Key Laboratory of Interface Science and Engineering in Advanced Materials, Ministry of Education, Taiyuan University of Technology, Taiyuan 030024, China. <sup>2</sup>Research Center of Advanced Materials Science and Technology, Taiyuan University of Technology, Taiyuan 030024, China.



Received: 12 March 2017 Accepted: 27 April 2017

Published online: 16 May 2017

## References

- Zhang Z-H, Liu W, Ju Z, Tiam Tan S, Ji Y, Kyaw Z et al (2014) Self-screening of the quantum confined Stark effect by the polarization induced bulk charges in the quantum barriers. *Appl Phys Lett* 104(24):243501
- Liu G, Zhao H, Zhang J, Park JH, Mawst LJ, Tansu N (2011) Selective area epitaxy of ultra-high density InGa<sub>N</sub> quantum dots by diblock copolymer lithography. *Nanoscale Res Lett* 6(1):342
- Zhang J, Tansu N (2013) Optical gain and laser characteristics of InGa<sub>N</sub> quantum wells on ternary InGa<sub>N</sub> substrates. *IEEE Photon J* 5(2):2600111
- Cao W, Biser JM, Ee YK, Li X-H, Tansu N, Chan HM et al (2011) Dislocation structure of GaN films grown on planar and nano-patterned sapphire. *J Appl Phys* 110(5):053505
- Lu T, Li S, Liu C, Zhang K, Xu Y, Tong J et al (2012) Advantages of GaN based light-emitting diodes with a p-InGa<sub>N</sub> hole reservoir layer. *Appl Phys Lett* 100(14):141106
- Jiang Y, Li Y, Li Y, Deng Z, Lu T, Ma Z et al (2015) Realization of high-luminous-efficiency InGa<sub>N</sub> light-emitting diodes in the “green gap” range. *Sci Rep* 5:10883
- Jin Y, Li Q, Li G, Chen M, Liu J, Zou Y et al (2014) Enhanced optical output power of blue light-emitting diodes with quasi-aligned gold nanoparticles. *Nanoscale Res Lett* 9(1):7
- Zhao Y, Yun F, Wang S, Feng L, Su X, Li Y et al (2016) Mechanism of hole injection enhancement in light-emitting diodes by inserting multiple hole-reservoir layers in electron blocking layer. *J Appl Phys* 119(10):105703
- Zhao H, Liu G, Tansu N (2010) Analysis of InGa<sub>N</sub>-delta-In<sub>N</sub> quantum wells for light-emitting diodes. *Appl Phys Lett* 97(13):131114
- Zhao H, Tansu N (2010) Optical gain characteristics of staggered InGa<sub>N</sub> quantum wells lasers. *J Appl Phys* 107(11):113110
- Rossow U, Hoffmann L, Bremers H, Buß ER, Ketzner F, Langer T et al (2015) Indium incorporation processes investigated by pulsed and continuous growth of ultrathin InGa<sub>N</sub> quantum wells. *J Cryst Growth* 414(4):49–55
- Du C, Ma Z, Zhou J, Lu T, Jiang Y, Zuo P et al (2014) Enhancing the quantum efficiency of InGa<sub>N</sub> yellow-green light-emitting diodes by growth interruption. *Appl Phys Lett* 105(7):071108
- Ting SM, Ramer JC, Florescu DI, Merai VN, Albert BE, Parekh A et al (2003) Morphological evolution of InGa<sub>N</sub>/Ga<sub>N</sub> quantum-well heterostructures grown by metalorganic chemical vapor deposition. *J Appl Phys* 94(3):1461–1467
- Kumar MS, Lee YS, Park JY, Chung SJ, Hong C-H, Suh E-K (2009) Surface morphological studies of green InGa<sub>N</sub>/Ga<sub>N</sub> multi-quantum wells grown by using MOCVD. *Mater Chem Phys* 113(1):192–195
- Cho HK, Lee JY, Kim CS, Yang GM (2002) Influence of strain relaxation on structural and optical characteristics of InGa<sub>N</sub>/Ga<sub>N</sub> multiple quantum wells with high indium composition. *J Appl Phys* 91(3):1166–1170
- Li X, Zhao DG, Yang J, Jiang DS, Liu ZS, Chen P et al (2016) Influence of InGa<sub>N</sub> growth rate on the localization states and optical properties of InGa<sub>N</sub>/Ga<sub>N</sub> multiple quantum wells. *Superlattices Microstruct* 97:186–192
- Lin Y, Zhou S, Wang W, Yang W, Qian H, Wang H et al (2015) Performance improvement of GaN-based light-emitting diodes grown on Si (111) substrates by controlling the reactor pressure for the GaN nucleation layer growth. *J Mater Chem C* 3(7):1484–1490
- Lu T, Ma Z, Du C, Fang Y, Wu H, Jiang Y et al (2014) Temperature-dependent photoluminescence in light-emitting diodes. *Sci Rep* 4:6131
- Lin T, Kuo HC, Jiang XD, Jiang XD, Feng ZC (2017) Recombination pathways in green InGa<sub>N</sub>/Ga<sub>N</sub> multiple quantum wells. *Nanoscale Res Lett* 12(1):137
- Scholz F, Off J, Fehrenbacher E, Gfrörer O, Brock T (2000) Investigations on structural properties of GaIn<sub>N</sub>-Ga<sub>N</sub> multi quantum well structures. *Phys Stat Sol (a)* 180(1):315–320
- Suihkonen S, Lang T, Svensk O, Sormunen J, Törmä PT, Sopanen M et al (2007) Control of the morphology of InGa<sub>N</sub>/Ga<sub>N</sub> quantum wells grown by metalorganic chemical vapor deposition. *J Cryst Growth* 300(2):324–329
- Daele BV, Tendeloo GV, Jacobs K, Moerman I, Leys MR (2004) Formation of metallic In in InGa<sub>N</sub>/Ga<sub>N</sub> multi-quantum wells. *Appl Phys Lett* 85(19):4379–4381
- Kumar MS, Park JY, Lee YS, Chung SJ, Hong C-H, Suh E-K (2007) Effect of barrier growth temperature on morphological evolution of green InGa<sub>N</sub>/Ga<sub>N</sub> multi-quantum well heterostructures. *J Phys D Appl Phys* 40(17):5050–5054
- Czernecki R, Grzanka E, Smalc-Koziorowska J, Grzanka S, Schiavon D, Targowski G et al (2015) Effect of hydrogen during growth of quantum barriers on the properties of InGa<sub>N</sub> quantum wells. *J Cryst Growth* 414:38–41
- Lv W, Wang L, Wang J, Hao Z, Luo Y (2012) InGa<sub>N</sub>/Ga<sub>N</sub> multilayer quantum dots yellow-green light-emitting diode with optimized Ga<sub>N</sub> barriers. *Nanoscale Res Lett* 7(1):617
- Ren P, Zhang N, Xue B, Liu Z, Wang J, Li J (2016) A novel usage of hydrogen treatment to improve the indium incorporation and internal quantum efficiency of green InGa<sub>N</sub>/Ga<sub>N</sub> multiple quantum wells simultaneously. *J Phys D Appl Phys* 49(17):175101
- Suihkonen S, Svensk O, Lang T, Lipsanen H, Odnoblyudov MA, Bougrov VE (2007) The effect of InGa<sub>N</sub>/Ga<sub>N</sub> MQW hydrogen treatment and threading dislocation optimization on Ga<sub>N</sub> LED efficiency. *J Cryst Growth* 298(1):740–743
- Czernecki R, Kret S, Kempisty P, Grzanka E, Plesiewicz J, Targowski G et al (2014) Influence of hydrogen and TMn on indium incorporation in MOVPE growth of InGa<sub>N</sub> layers. *J Cryst Growth* 402(402):330–336
- Hu Y-L, Farrell RM, Neufeld CJ, Iza M, Cruz S, Pfaff N et al (2012) Effect of quantum well cap layer thickness on the microstructure and performance of InGa<sub>N</sub>/Ga<sub>N</sub> solar cells. *Appl Phys Lett* 100(16):161101
- Pan Z, Wang YT, Zhuang Y, Lin YW, Zhou ZQ, Li LH et al (1999) Investigation of periodicity fluctuations in strained (Ga<sub>N</sub>As)<sub>m</sub>(GaAs)<sub>n</sub> superlattices by the kinematical simulation of x-ray diffraction. *Appl Phys Lett* 75(2):223–225
- Lin F, Xiang N, Chen P, Chow SY, Chua SJ (2008) Investigation of the V-pit related morphological and optical properties of InGa<sub>N</sub>/Ga<sub>N</sub> multiple quantum wells. *J Appl Phys* 103(4):043508
- Chen Y, Takeuchi T, Amano H, Akasaki I, Yamada N, Kaneko Y et al (1998) Pit formation in GaIn<sub>N</sub> quantum wells. *Appl Phys Lett* 72(6):710–712
- Liliental-Weber Z, Chen Y, Ruvimov S, Washburn J (1997) Formation mechanism of nanotubes in Ga<sub>N</sub>. *Phys Rev Lett* 79(15):2835–2838
- Sun CJ, Zubair Anwar M, Chen Q, Yang JW, Asif Khan M, Shur MS et al (1997) Quantum shift of band-edge stimulated emission in InGa<sub>N</sub>-Ga<sub>N</sub> multiple quantum well light-emitting diodes. *Appl Phys Lett* 70(22):2978–2980
- Wu XH, Elsass CR, Abare A, Mack M, Keller S, Petroff PM et al (1998) Structural origin of V-defects and correlation with localized excitonic centers in InGa<sub>N</sub>/Ga<sub>N</sub> multiple quantum wells. *Appl Phys Lett* 72(6):692–694
- Morishita Y, Nomura Y, Goto S, Katayama Y (1995) Effect of hydrogen on the surface-diffusion length of Ga adatoms during molecular-beam epitaxy. *Appl Phys Lett* 67(17):2500–2502
- Shiojiri M, Chuo CC, Hsu JT, Yang JR, Saijo H (2006) Structure and formation mechanism of V defects in multiple InGa<sub>N</sub> / Ga<sub>N</sub> quantumwell layers. *J Appl Phys* 99(7):073505
- Wang HX, Amijima Y, Ishihama Y, Sakai S (2001) Influence of carrier gas on the morphology and structure of Ga<sub>N</sub> layers grown on sapphire substrate by six-wafer metal organic chemical vapor deposition system. *J Cryst Growth* 233(7):681–686
- Koukita A, Taki T, Takahashi N, Seki H (1999) Thermodynamic study on the role of hydrogen during the MOVPE growth of group III nitrides. *J Cryst Growth* 197(1):99–105
- Sangwal K (1987) Etching of crystals: theory, experiment and application
- Yu C-C, Chu C-F, Tsai J-Y, Huang HW, Hsueh T-H, Lin C-F et al (2002) Gallium nitride nanorods fabricated by inductively coupled plasma reactive ion etching. *Jpn J Appl Phys* 41(41):L910–L912
- Yeh Y-H, Chen K-M, Wu Y-H, Hsu Y-C, Yu T-Y, Lee W-I (2011) Hydrogen etching of Ga<sub>N</sub> and its application to produce free-standing Ga<sub>N</sub> thick films. *J Cryst Growth* 333(1):16–19
- Yeh Y-H, Chen K-M, Wu Y-H, Hsu Y-C, Lee W-I (2011) Hydrogen etching on the surface of Ga<sub>N</sub> for producing patterned structures. *J Cryst Growth* 314(1):9–12
- Hiramatsu K, Nishiyama K, Motogaito A, Miyake H, Iyechika Y, Maeda T (1999) Recent developments in selective area growth and epitaxial lateral overgrowth of III-nitrides. *Phys Stat Sol (a)* 176(1):535–543
- Tiginyanu I, Stevens-Kalceff MA, Sarua A, Braniste T, Monaco E, Popa V et al (2016) Self-organized three-dimensional nanostructured architectures in bulk Ga<sub>N</sub> generated by spatial modulation of doping. *ECS J Solid St Sci Technol* 5(5):218–227
- Bai J, Wang T, Sakai S (2000) Influence of the quantum-well thickness on the radiative recombination of InGa<sub>N</sub>/Ga<sub>N</sub> quantum well structures. *J Appl Phys* 88(8):4729–4733
- Meneghini M, Trivellini N, Pavesi M, Manfredi M, Zehnder U, Hahn B et al (2009) Leakage current and reverse-bias luminescence in InGa<sub>N</sub>-based light-emitting diodes. *Appl Phys Lett* 95(17):173507



48. Shapiro NA, Feick H, Hong W, Cich M, Armitage R, Weber ER et al (2003) Luminescence energy and carrier lifetime in InGaN/GaN quantum wells as a function of applied biaxial strain. *J Appl Phys* 94(7):4520–4529
49. Tawfik WZ, Song J, Lee JJ, Ha JS, Ryu S-W, Choi HS et al (2013) Effect of external tensile stress on blue InGaN/GaN multi-quantum-well light-emitting diode. *Appl Surf Sci* 283(14):727–731
50. Moon Y-T, Kim D-J, Song K-M, Kim D-W, Yi M-S, Noh D-Y et al (2000) Effect of growth interruption and the introduction of H<sub>2</sub> on the growth of InGaN/GaN multiple quantum wells. *J Vac Sci Technol B* 18(6):2631–2634
51. Piner EL, Behbehani MK, El-masry NA, Roberts JC, McIntosh FG, Bedair SM (1997) Impurity dependence on hydrogen and ammonia flow rates in InGaN bulk films. *Appl Phys Lett* 71(14):2023–2025

**Submit your manuscript to a SpringerOpen<sup>®</sup> journal and benefit from:**

- ▶ Convenient online submission
- ▶ Rigorous peer review
- ▶ Immediate publication on acceptance
- ▶ Open access: articles freely available online
- ▶ High visibility within the field
- ▶ Retaining the copyright to your article

---

Submit your next manuscript at ▶ [springeropen.com](http://springeropen.com)

---